Published in final edited form as:
Cancer Discov. 2013 August ; 3(8): 894–907. doi:10.1158/2159-8290.CD-13-0011.

Autophagy opposes p53-mediated tumor barrier to facilitate tumorigenesis in a model of *PALB2*-associated hereditary breast cancer

Yanying Huo[1,2], **Hong Cai**[1,2], **Irina Teplova**[1], **Christian Bowman-Colin**[3], **Guanghua Chen**[1], **Sandy Price**[1], **Nicola Barnard**[4], **Shridar Ganesan**[1,5], **Vassiliki Karantza**[1,5], **Eileen White**[1,6], and **Bing Xia**[1,2]

[1]The Cancer Institute of New Jersey, 195 Little Albany Street, New Brunswick, NJ 08903

[2]Department of Radiation Oncology, Robert Wood Johnson Medical School, University of Medicine and Dentistry of New Jersey, New Brunswick, NJ 08903

[3]Department of Cancer Biology, Dana-Farber Cancer Institute, 450 Brookline Avenue, Boston, MA, 02115

[4]Department of Pathology, Robert Wood Johnson Medical School, New Brunswick, NJ 08903

[5]Department of Medicine, Robert Wood Johnson Medical School, New Brunswick, NJ 08903

[6]Department of Molecular Biology and Biochemistry, Rutgers University, 604 Allison Road, Piscataway, NJ 08854

Abstract

Hereditary breast cancers stem from germline mutations in susceptibility genes such as *BRCA1*, *BRCA2* and *PALB2*, whose products function in the DNA damage response and redox regulation. Autophagy is an intracellular waste disposal and stress mitigation mechanism important for alleviating oxidative stress and DNA damage response activation; it can either suppress or promote cancer, but its role in breast cancer is unknown. Here we show that, similar to *Brca1* and *Brca2*, ablation of *Palb2* in mouse mammary gland resulted in tumor development with long latency and the tumors harbored mutations in *Trp53*. Interestingly, impaired autophagy, due to monoallelic loss of the essential autophagy gene *Becn1*, reduced *Palb2*-associated mammary tumorigenesis in *Trp53*-wild type but not conditionally null background. These results indicate that, in the face of DNA damage and oxidative stress elicited by PALB2 loss, p53 is a barrier to cancer development, whereas autophagy facilitates cell survival and tumorigenesis.

Introduction

About 5–10% of breast cancer occurs in the form of inherited predisposition in certain high-risk families in which women tend to develop the disease at higher frequencies and at younger ages than the general population. Interestingly, nearly all of the known familial breast cancer genes function, at least in part, in the repair and/or signaling response to DNA damage, particularly double strand breaks (DSBs) (1). In addition, several of the susceptibility genes, e.g. *BRCA1*, *PALB2*, *TP53* and *ATM*, etc., also share a function in

Corresponding author: Bing Xia, Department of Radiation Oncology, The Cancer Institute of New Jersey, 195 Little Albany Street, New Brunswick, NJ 08903, Phone: 732-235-7410, xiabi@umdnj.edu.
Y. Huo and H. Cai share the first authorship.

Disclosure of Potential Conflicts of Interest
No potential conflicts of interest were disclosed by the authors.

reducing cellular levels of reactive oxygen species (ROS), which cause genome damage and promote tumorigenesis (2–6). Thus, a major fraction of hereditary breast cancer appears to result from a common root, namely genome instability.

BRCA1 and BRCA2 perform key functions in genome stability maintenance by promoting faithful repair of DSBs by homologous recombination (HR) and other relevant processes (7, 8). We discovered PALB2 as a major BRCA2 binding partner that controls its chromatin association and function in HR (9). Subsequent work established PALB2 as a BRCA2-like tumor suppressor that is mutated in familial breast and pancreatic cancers as well as Fanconi anemia (10–16). More recently, PALB2 was shown to directly bind BRCA1 as well and link BRCA1 and BRCA2 in HR repair (17, 18). Importantly, multiple patient-derived missense mutations that abrogate PALB2 binding have been identified in both BRCA1 and BRCA2 and shown to disable their HR-repair function (9, 18), indicating that the three proteins function together in a BRCA complex/pathway to promote HR and suppress tumor development.

Contrary to an expectation that mice lacking *Brca1* or *Brca2* may develop breast cancer, complete knockout of either gene was found to result in early embryonic lethality (19). It was then realized that these genes were indispensable for HR, which is essential not only for tumor suppression but also for mammalian development. Consistent with a role of PALB2 as a linker between BRCA1 and BRCA2 in HR, systemic knockout of *Palb2* in mouse resulted in phenotypes similar to that of *Brca1* and *Brca2*, including early embryonic lethality and induction of the cyclin-dependent kinase inhibitor p21 (20, 21).

The p53 transcription program plays essential roles in regulating many critical aspects of cell and tissue physiology that collectively prevent tumorigenesis. Virtually 100% of *BRCA1*-associated human breast cancers harbor mutations or deletions of the *TP53* gene, and *BRCA2* and *PALB2* tumors also frequently contain *TP53* mutations (11, 22, 23). Similarly, somatic mutations in *Trp53* are frequently found in mammary tumors that develop in *Brca1* and *Brca2* conditional knockout (CKO) mouse models (24, 25), and *Trp53* co-deletion or heterozygosity strongly accelerated mammary gland tumor development in all *Brca1* and *Brca2* models tested (26–30). Moreover, loss of p53 partially rescues the embryonic lethality and developmental defect caused by the knockout of each of the 3 genes (21, 31). The evidence indicates that inactivation of the p53 pathway may be a prerequisite for mammary epithelial cells (MECs) to survive the DNA damage and escape the resulting cell cycle checkpoint following BRCA1/2 loss and perhaps also that of PALB2.

Autophagy is an intracellular waste disposal and recycling process whereby damaged organelles and certain proteins are engulfed in double-membrane vesicles (autophagosomes) and delivered to lysosomes for degradation (32). By eliminating damaged mitochondria and toxic protein aggregates and perhaps through other unknown mechanisms, autophagy mitigates oxidative stress and promotes genome stability, thereby suppressing tumorigenesis (33–35). Indeed, monoallelic loss of the essential autophagy gene *Beclin 1* (*Becn1*) in mice leads to increased tumor development at old ages (35–37). Interestingly, autophagy has been shown to be upregulated in RAS-driven cancers, and these cancer cells appear to be “addicted” to and rely on autophagy for survival (38, 39). Thus, autophagy can also facilitate tumor development, presumably by mitigating oxidative stress and promoting tumor cell fitness and nutrient recycling (40, 41).

In this study, we generated and characterized a model of *PALB2*-associated breast cancer. Moreover, using this model we explored the role of p53 and autophagy in breast cancer associated with oxidative stress and DNA damage. Our results demonstrate that an inactivation of p53 is critical for most, if not all, *Palb2*-associated tumorigenesis, that

autophagy facilitates the development of such breast cancer by promoting tumor cell survival and that the effect of autophagy on mammary tumorigenesis is influenced by p53 status.

Results

Mammary Tumor Development in *Palb2* Conditional Knockout Mice

To gain new insights into PALB2-mediated tumor suppression, we targeted the mouse *Palb2* gene by inserting loxP sites into introns 1 and 3 (Fig. 1A). Cre-mediated excision of exons 2 and 3 would render exon 4 out of frame and result in a functionally null *Palb2* gene (42). To inactivate *Palb2* in the mammary gland, *Palb2*-floxed animals were crossed with mice bearing a *Cre* transgene driven by the mammary gland specific promoter of whey acidic protein (*Wap-cre*) (43). The resulting females were mated to undergo two rounds of pregnancy and lactation to induce maximal Cre expression in alveolar MECs, and then monitored for tumor development. As shown in Fig. 1B, 19 out of 29 (66%) of mice with MEC-specific knockout of *Palb2* developed 20 mammary tumors (T_{50}=607 days), directly demonstrating that *Palb2* acts as a tumor suppressor in the mammary gland. None of the 18 control animals (with *Wap-cre*) developed mammary tumors.

Characteristics of *Palb2*-associated Mammary Tumors

Eighteen of the 20 mammary tumors that developed in the *Palb2*$^{f/f}$;*Wap-cre* mice were analyzed for histology and immunophenotypes. Four characteristic histological types were observed- solid (poorly differentiated adenocarcinoma), tubular (well differentiated adenocarcinoma), sarcomatoid (post epithelial to mesenchymal transition (EMT)) and adenosquamous (adenocarcinoma with squamous differentiation) (Fig. 1C). Ten of the 18 tumors (56%) were mostly solid with varying degrees of tubule formation, one was largely tubular, 3 were mostly sarcomatoid, 2 had squamous differentiation and the remaining 2 were mixtures of solid and sarcomatoid with ongoing EMT (Table 1). Necrosis was a common feature in solid areas but rarely seen in other areas or tumors. Nuclear grades were generally high except in the tubular areas of a few tumors. Although well-defined pushing margins were observed for all of the tumors, at least 15 of them were found to have invasive borders in one or more areas (Fig. 1C and S1). Moreover, 10 out of the 18 tumors appeared to have invaded into skin or muscle at the time of collection. Additional views of histology are shown in Fig. S1.

The status of the estrogen receptor (ER) and progesterone receptor (PR) in the 18 tumors was analyzed by immunohistochemistry (IHC) (Fig. 2A). Eight (44%) tumors showed positive ER staining and 4 (22%) were PR-positive (Table 1). For ER, the positive tumors generally showed nuclear staining in greater than 30% of the cells but the overall signal strength appeared to be weaker than what is commonly seen in typical human ER+ cancers. Similar findings were made for PR except that higher background staining was observed in approximately half of the tumors, in which case a "-" status was assigned unless some of the cells showed strong nuclear signal clearly above the background. Taken together, these results demonstrates that somatic deletion of *Palb2* driven by *Wap-cre* can give rise to both ER+ and ER− mammary tumors, a scenario similar to human *PALB2*-associated breast cancers (10).

Role of p53 in *Palb2*-associated Mouse Mammary Tumors

The prevalence of *TP53* mutations in *BRCA*- and *PALB2*-associated human breast tumors led us to sequence the *Trp53* gene (cDNA) in tumors that arose from *Palb2*$^{f/f}$;*Wap-cre* mice. Among the 14 tumors analyzed, 9 (64%) contained missense mutations or internal deletions, 4 were wild type and the remaining one did not yield cDNA, presumably due to biallelic

deletion or extremely low mRNA expression level (Table 1). This finding suggests that loss of p53 function is important for the development of *Palb2*-associated mammary tumors. In the 4 tumors with a wild type *Trp53* transcript, it is still possible that the p53 pathway may be rendered nonfunctional by other mechanisms, such as hyperactivation of MDM2.

To further understand the status of p53 in the tumors, we analyzed its protein levels using IHC (Fig. 2B). Nine (50%) of the 18 tumors were positive, including all of the 7 tumors with missense mutations (Table 1). As expected, the 2 tumors with intragenic deletions/frameshift mutations both showed completely negative staining. Three of the 4 tumors with wt *Trp53* were negative but one was, surprisingly, strongly positive (#882). Although it is unclear whether the p53 downstream pathway is active in this particular tumor, our findings overall indicate that loss of normal p53 function is critical for the development of *Palb2*-associated mammary tumors.

To study the genetic interaction between *Palb2* and *Trp53*, we introduced a floxed *Trp53* allele (26) into our model. As shown in Fig. 1B, combined deletion of *Palb2* and *Trp53* in MECs led to highly efficient tumor development that is much faster than that caused by *Palb2* single deletion. The median tumor latency of the double CKO mice was also slightly shorter than that of the *Trp53* single CKO mice (T_{50}=246 vs 289 days), suggesting that two genes may synergistically suppress breast cancer development. However, the difference did not reach statistical significance (p=0.0647, log-rank analysis). Additionally, we also monitored a small number (n=9) of $Palb2^{w/w}$;$Trp53^{f/w}$;*Wap-cre* females, and 7 of them developed mammary tumors with latencies from 466 to 736 days, which were in the similar range as tumors arising in $Palb2^{f/f}$;$Trp53^{w/w}$;*Wap-cre* mice.

DNA Damage in *Palb2*-null Tumor Cells and Their Sensitivity to DNA Damaging Agents

Given the role of PALB2 in DNA repair, we assessed the extent of endogenous DNA damage in tumors by IHC analysis of γH2A.X, a marker of DSBs (Fig. 2C). Thirteen (72%) of them showed γH2A.X staining regardless of *Trp53* status, indicative of the existence of unrepaired DSBs (Table 1). In contrast, little to no staining was detected in tumors arising from $Palb2^{w/w}$;$Trp53^{f/w}$;*Wap-cre* mice, which developed with similar latency (Fig. 2C). Consistent with our recent finding that PALB2 plays a role in the oxidative stress response (4), the *Palb2*-null tumors were found to have much higher levels of oxidative DNA damage as revealed by IHC staining of 8-oxo-dG, a marker of such damage, as compared with the above-noted *Trp53*-associated tumors (Fig. 2C).

We have shown earlier that *PALB2*-null FA fibroblasts, like *BRCA1*- and *BRCA2*-null cells, are sensitive to agents that target HR-mediated DSB repair, such as mitomycin C (MMC) and poly (ADP-ribose) polymerase (PARP) inhibitors (14, 44). However, to our knowledge no human *PALB2*-null breast cancer cells have been established. Thus, to better understand the function and "druggability" of PALB2 we attempted to generate cell lines from the mouse mammary tumors. Several attempts were made to generate cell lines from *Palb2*-single-null tumors, but only one useful line (PF741) was successfully established, which retained a wt *Trp53* gene. In contrast, multiple lines were established from *Trp53*-single-null (*Palb2*-wt) and *Palb2*/*Trp53*-double-null tumors.

Above cells were tested for their ability to repair DNA damage elicited by olaparib, a PARP inhibitor, and MMC. Interestingly, the *Palb2*-null cells contained more DSBs as revealed by γH2A.X immunofluorescence (IF) even in the absence of drugs, which was particularly evident in the *Palb2*/*Trp53*-double-null cells (Figs. 3A and S2). By 3 hr following treatment, both agents resulted in increased γH2A.X staining signal in all 3 cell types, and distinct RAD51 foci colocalizing with those of γH2A.X was observed in *Palb2*-wt cells but not in either of the *Palb2*-null cells. By 8 hr post treatment, γH2A.X signals had returned to pre-

treatment levels in the *Palb2*-wt cells, whereas the signals persisted in both types of *Palb2*-null cells. By this time, RAD51 foci had largely disappeared in the *Palb2*-wt cells, and *Palb2*-single-null cells showed a diffuse RAD51 staining pattern. Another p53-single-null (control) and 2 additional *Palb2*/*Trp53*-double-null cell lines were tested in parallel and the results were essentially the same.

Next, we performed neutral comet assays to further assess the levels of DNA breaks in the 6 cell lines. Compared with the 2 *Palb2*-wt cells, all 4 *Palb2*-null cells showed substantially higher levels of DNA breaks before drug treatment (Fig. 3B and S2), indicative of a significant defect in the repair of DNA breaks resulting from endogenous factors, such as collapse of replication forks, etc. At 3 hr after drug treatment, increased DNA fragmentation was seen in all cells. By 8 hr post treatment, the levels of DNA breaks were found to have decreased in the *Palb2*-wt cells but not the *Palb2*-null cells (Figs. 3B and S2), again indicating an inability of the mutant cells to execute HR-based repair. Consistently, both types of *Palb2*-deficient cells were hypersensitive to both agents (Fig. 3C–D). The deletion of the respective proteins in the cell lines were confirmed by Western blotting (Fig. 3E). Collectively, these results further underscore the critical role of PALB2 in HR repair and support the applicability of PARP inhibitors and DNA crosslinkers for *PALB2*-associated cancers.

Senescence and Apoptosis upon *Palb2* Deletion and the Rescue by Co-deletion of *Trp53*

To test the immediate consequence of PALB2 loss in primary cells and the role of p53 in this process, we generated mouse embryonic fibroblasts (MEFs) from $Palb2^{f/f}$ and $Palb2^{f/f}$;$Trp53^{f/f}$ mice. After the cells were infected with a Cre-encoding retrovirus to induce gene deletion and subjected to selection, virtually complete loss of the respective proteins was observed (Fig. 4A–B). As expected, *Palb2*-null MEFs showed much increased endogenous DSBs as evidenced by nuclear foci formation of 53BP1 (Fig. 4C). γH2A.X foci were not counted in all experiments. However, when we co-stained γH2A.X with 53BP1, all 53BP1-positive cells were found to be positive for γH2A.X whereas some cells showing multiple but weakly stained γH2A.X foci did not display distinct 53BP1 foci (Fig. S3). Thus, the actual extent of DNA breaks in the cells should be even greater.

Consistent with our previous finding that PALB2 promotes the nuclear accumulation and function of the antioxidant transcription factor NRF2 (4), the protein was localized mostly in the nucleus in *Palb2*-wild type MEFs but showed a diffuse staining pattern in *Palb2*-null MEFs (Fig. 4D). Accordingly, *Palb2*-null MEFs had significantly higher ROS levels throughout the experimental period (Fig. 4E). Together with the fact that *Palb2*-null tumor cells contained higher levels of oxidative DNA damage (Fig. 2C), these results further underscore the importance of PALB2 in cellular defense against oxidative stress.

Notably, starting from passage 2, large numbers of *Palb2*-null MEFs appeared flat and enlarged, stained positive for beta-galactosidase (β-gal) and displayed poor growth (Fig. 4F–H), indicating that the cells were entering senescence. Moreover, an Annexin V assay revealed apoptosis occurring in a substantial fraction of the cells (Fig. 4I). Co-deletion of *Trp53* completely rescued the slow growth, senescence and apoptosis phenotypes that resulted from *Palb2* deletion. These observations indicate that loss of p53 is able to allow cells to overcome growth arrest or apoptosis induced by DNA damage and oxidative stress after PALB2 loss.

Effect of *Becn1* Heterozygosity on *Palb2*-associated Mammary Tumorigenesis

Autophagy is particularly important for mitigating oxidative stress and suppressing DNA damage response activation during stresses. In addition, recent studies have demonstrated

that autophagy can also facilitate cellular senescence (45). Therefore, we suspected that autophagy might play a role in *PALB2*-associated breast cancer development. To address this, we crossed the *Palb2*$^{f/f}$;*Wap-cre* and *Palb2*$^{f/f}$;*Trp53*$^{f/f}$;*Wap-cre* mice to *Becn1*$^{+/-}$ mice (36). As shown in Fig. 5A, allelic loss of *Becn1* significantly delayed mammary tumor formation in *Palb2*$^{f/f}$;*Wap-cre* animals (p=0.0035, log-rank analysis). Moreover, only 7 of the 26 *Becn1*$^{+/-}$ animals developed mammary tumors. However, it did not affect tumorigenesis due to combined MEC-specific loss of *Palb2* and *Trp53*, suggesting that the suppression of *Palb2*-mediated tumorigenesis upon allelic loss of *Becn1* is mediated by p53.

The 8 tumors that formed in the 7 *Palb2*$^{f/f}$;*Wap-cre;Becn1*$^{+/-}$ mice were similar to their *Becn1*$^{+/+}$ counterparts in terms of histology and DNA damage levels (Table 1). Two (25%) of them were marginally positive for ER, showing weak staining signals that were only seen in some areas of the tumors. Moreover, only one of the 6 tumors (16.7%) sequenced was found to have a *Trp53* mutation, as compared with the 64% mutation rate of the *Becn1*$^{+/+}$ tumors. These findings imply that a defect in autophagy may force a different path of tumor evolution following PALB2 loss. Due to the small number of *Becn1*$^{+/-}$ tumors obtained in this work, a larger study may be needed to confirm the results and address the potential mechanisms.

Autophagy and Apoptosis in the *Palb2*-deficient Mammary Tumors

The finding that allelic loss of *Becn1* suppressed *Palb2*-associated mammary tumorigenesis by a p53-depedent mechanism suggests that autophagy facilitates tumor development. To assess the levels of autophagy activity in the mammary tumors, we analyzed 12 tumor samples (6 *Becn1*$^{+/+}$ and 6 *Becn1*$^{+/-}$) using electron microscopy. A number of autophagosomes were identified (Fig. 5B), indicating that autophagy indeed occurs in *Palb2*-associated breast cancer even in the absence of external stress. Notably, autophagosomes were observed in 5 of the 6 *Becn*$^{+/+}$ tumors but in only one of the 6 *Becn*$^{+/-}$ tumors, suggesting that allelic loss of *Becn1* caused a partial, but appreciable, impairment of autophagy in the setting used. To further confirm the autophagy defect in the *Becn1*$^{+/-}$ tumors, we compared the levels of p62 (SQSTM1), which is an important substrate for autophagy and accumulates when autophagy is impaired (35). When necrotic areas were excluded, all *Becn1*$^{+/+}$ tumors exhibited weak or virtually no staining signal, whereas distinct areas of strong staining were observed in tumors arising from *Palb2*$^{f/f}$*;Wap-cre;Becn1*$^{+/-}$ mice (Fig. 5C). In mammary tumors from *Palb2*$^{f/f}$*;Trp53*$^{f/f}$*;Wap-cre;Becn1*$^{+/-}$ animals, positive p62 staining was observed, but was markedly weaker than in mammary tumors arising from *Palb2f/f;Wap-cre;Becn1*$^{+/-}$ mice.

Next, we analyzed the levels of cleaved (activated) caspase-3, which marks apoptotic cells, in the tumor tissues. As in the case of p62, tumors from *Palb2*$^{f/f}$*;Wap-cre;Becn1*$^{+/+}$ mice showed weak or no cleaved caspase-3 staining across non-necrotic areas, whereas pockets of positive staining were found in tumors that developed in *Palb2*$^{f/f}$*;Wap-cre;Becn1*$^{+/-}$ animals (Fig. 5D). In the *Palb2;Trp53*-doubly-deleted tumors, the staining was all negative regardless of *Becn1* status. Thus, combined deficits in DNA repair and autophagy appeared to elevate p53-dependent apoptosis in *Palb2*$^{-/-}$*;Becn1*$^{+/-}$ mammary tumor cells. To further address the potential correlation between autophagy defect and cell death (apoptosis) in *Palb2*-associated mammary tumors, we analyzed 6 tumors with wild type *Trp53* (3 *Palb2*$^{-/-}$*;Becn1*$^{+/-}$ and 3 *Palb2*$^{-/-}$*; Becn1*$^{+/+}$) by IHC for p62, LC3B (another autophagy substrate) and cleaved caspase-3. As shown in Fig. S4, the 3 *Becn*$^{+/-}$ tumors stained positive for all 3 markers, whereas the 3 *Becn1*$^{+/+}$ tumors showed virtually no staining.

Discussion

We demonstrated that ablation of *Palb2* in MECs led to mammary tumor development with a median latency of 607 days. The tumors displayed diverse histology but were generally high grade and invasive. With respect to hormone receptors, 44% of tumors analyzed showed positive ER staining and 22% were PR-positive (Table 1). In comparison, human *PALB2* cancers are also generally high grade, whereas ER/PR status of the tumors appears to vary significantly depending on mutations and/or populations (10). Overall, approximately 40% of human *PALB2* tumors were triple negative for ER, PR and HER2, putting the clinical phenotypes of *PALB2* between *BRCA1* and *BRCA2* (10, 46). Thus, although our model shows somewhat lower positivity for ER and PR, it still recapitulates some key features of the human *PALB2* disease, namely the high grade and intermediate ER positivity.

Among the numerous *Brca1*- and *Brca2*- CKO breast cancer models that have been reported (19, 47), the most comparable to this model are the *Wap-cre*-driven ones reported by Ludwig and colleagues (24, 25). In these studies, somatic deletion of *Brca1* resulted in tumors that were 91% (19/21) ER-negative and basal-like; while *Brca2* ablation produced tumors that were 50% (15/30) ER+ and 7% (2/30) PR+. Thus, the 44% ER+ and 22% PR+ rates of the *Palb2* mammary tumors in this study are more phenotypically similar to *Brca2*-associated ones, which is consistent with what appears to be a much stronger physical association of PALB2 with BRCA2 than with BRCA1 (9, 18).

Median latencies of 512 and 508 days were reported for the above $Brca1^{f/f}$;*Wap-cre and* $Brca2^{f/-}$;*Wap-cre* mice, respectively (24, 28). In a separate $Brca1^{f/-}$;*Wap-cre* model, mammary tumors were found in 2 out of 13 animals sacrificed between ages of 10–13 months (27). Given the differences in backgrounds and experimental settings, it is impossible to strictly compare these latencies with that of the present *Palb2* model. Still, the long latencies in all 4 models indicate that there is a strong barrier to tumor development in mammary epithelial cells (MECs) that have suffered the loss of any one of these tumor suppressor proteins. As noted before, accumulating evidence from both human and mouse studies suggest that the barrier may be mostly enforced by p53. Our finding that the majority of the *Palb2*-associated tumors analyzed here (9/14) were *Trp53*-mutated lends further support to the above notion.

The most prominent molecular function shared by BRCA1/2 and PALB2 proteins is their role in HR, which is the major mechanism to repair the type of DSBs that inevitably arise during normal DNA replication. Upon loss of any of these proteins, an inability of cells to prevent and repair collapsed replication forks leads to DSB accumulation and a DNA damage response that presumably activates p53. Depending on circumstances and the extent of p53 activation, cells may undergo G1/S arrest, senescence and/or apoptosis. It still remains to be seen which one(s) is the predominant consequence of BRCA or PALB2 loss in MECs in vivo. This knowledge is important for understanding the developmental path, as well as tissue specificity, of *BRCA*- and *PALB2*-associated cancers.

Based on existing knowledge and results obtained in this study, we propose a model of *PALB2*-associated hereditary breast cancer development as illustrated in Fig. 6. Under normal conditions, PALB2 functions together with BRCA1 and BRCA2 to maintain genome stability and cellular homeostasis to suppress cancer development. When PALB2 is lost, increased DNA damage and ROS cause activation of p53, which induces growth inhibition and perhaps senescence or apoptosis thereby suppressing tumor formation. Under such adverse conditions, autophagy facilitates cell survival and growth, which allows *PALB2*-null cells to accumulate further mutations and evolve into cancer cells. When autophagy is

defective, increased cell death occurs and the potential for tumor development is reduced. If PALB2 is lost in a cell with already mutated p53, highly efficient tumor formation occurs under both normal and low autophagy conditions.

The role of p53 in regulating autophagy has been reported by multiple groups and appears to be complex. In particular, one study showed that nuclear p53 promotes autophagy by inducing relevant gene expression whereas cytoplasmic p53 inhibits autophagy (48). In the present study, allelic loss of *Becn1* did not produce any difference in tumor formation in mice with *Palb2;Trp53* double deletion in MECs. This finding may have at least two different implications. First, the strong growth advantage conferred by a complete p53 loss may override the reduced fitness elicited by impaired autophagy in $Palb2^{-/-}$ MECs or tumor cells. Second, p53 may negatively regulate autophagy in these cells so that loss of p53 leads to a compensation of autophagy function. However, it is important to note that real world cancers mostly harbor *TP53* point mutations combined with loss of heterozygosity (LOH) instead of biallelic deletions, and it is known that point mutants may possess both loss and gain of functions. Therefore, the actual effect of *TP53* mutations on the impact of autophagy on cancer may be variable and again context-dependent.

Our finding is consistent with a recent study which found that allelic loss of *Becn1* delayed tumor development in *ATM*-deficient mice (3). However, while the above study suggests that *Becn1* heterozygosity leads to a restoration of mitochondria health damaged by *ATM* deficiency, no gross difference was noted in mitochondria of the tumor samples analyzed by EM in the present study. Still, the $Becn^{+/-}$ tumors appeared to contain fewer vesiculated mitochondria and perhaps more fused ones than the $Becn1^{+/+}$ tumors (Fig. S5). Yet, due to the small number of samples analyzed and the high degree of heterogeneity within each sample, it is unfeasible to draw any conclusions from the current study. Further investigation is needed to understand the potential involvement of mitochondria physiology in hereditary breast cancer.

Inhibiting autophagy as a potential cancer therapy has gained increasing attention. In this study, $Palb2^{-/-};Becn1^{+/-}$ tumors had reduced incidence and also seemed to grow slower compared with the corresponding $Becn1^{+/+}$ tumors. Consistently, such ($Becn1^{+/-}$) tumors were found to contain areas undergoing apoptosis. These results suggest that rational autophagy inhibition may selectively kill *PALB2*-deficient tumor cells. Given the close relationship and functional similarity between PALB2 and BRCA1/2, the same notion may apply to *BRCA*-deficient tumor cells as well.

Materials and Methods

To create a *Palb2* conditional knockout mouse model, we targeted the *Palb2* locus and generated a strain in which exons 2 and 3 of the gene are flanked by loxP sites (42). The $Palb2^{flox/flox}$ mice were crossed to strains carrying $Trp53^{flox2\text{-}10}$ (26), *Becn1*-KO (36) and *Wap-cre* (43) alleles to generate all the genotypes in this study. Females of desired genotypes were mated to go through two rounds of pregnancy and lactation to induce *Wap-cre* expression and then monitored for tumor development. Tumors were collected when they reached ~1.0 cm in diameter. Primary mouse embryo fibroblasts (MEFs) were generated from E13.5 embryos. All experimental procedures involving animals were conducted in accordance with policies set forth by the Institutional Animal Care and Use Committee (IACUC) of the Robert Wood Johnson Medical School and under the protocol numbers I08-073-9 and I11-029-5. To delete *Palb2* and *Trp53* genes in MEFs, freshly generated cells with floxed alleles were infected with a Cre-encoding retrovirus and selected with puromycin. Mammary tumor cells were generated from tumor specimens dissociated with collagenase. Olaparib and mitomycin C (MMC) sensitivities were determined by the

CellTiter Glo® cell proliferation assay (Promega). Levels of reactive oxygen species (ROS) were measured using the DCF (2′,7′-Dichlorofluorescin diacetate) assay. Cellular senescence and apoptosis were determined using the senescence-associated β-galactosidase (SA-β-gal) assay and Annexin V assay, respectively. Western blotting and immunofluorescence (IF) staining were performed using standard protocols. Neutral comet assay was performed using the CometAssay® kit from Trevigen following manufacturer's protocol. For details see online methods in the Supporting Information (SI).

Supplementary Material

Refer to Web version on PubMed Central for supplementary material.

Acknowledgments

We thank Drs. David Livingston and Chrysi Kanellopoulou for supporting the initial stage of the work and for their critical comments on the manuscript. We also thank Dr. Shoreh Miller for valuable assistance in mouse breeding. This work was supported by the National Cancer Institute (R01CA138804 to B.X.), the American Cancer Society (RSG #TBG-119822 to B.X.) and The Cancer Institute of New Jersey (to B.X.).

References

1. Walsh T, King MC. Ten genes for inherited breast cancer. Cancer Cell. 2007; 11:103–5. [PubMed: 17292821]
2. Saha T, Rih JK, Rosen EM. BRCA1 down-regulates cellular levels of reactive oxygen species. FEBS letters. 2009; 583:1535–43. [PubMed: 19364506]
3. Valentin-Vega YA, Maclean KH, Tait-Mulder J, Milasta S, Steeves M, Dorsey FC, et al. Mitochondrial dysfunction in ataxia-telangiectasia. Blood. 2012; 119:1490–500. [PubMed: 22144182]
4. Ma J, Cai H, Wu T, Sobhian B, Huo Y, Alcivar A, et al. PALB2 interacts with KEAP1 to promote NRF2 nuclear accumulation and function. Molecular and cellular biology. 2012; 32:1506–17. [PubMed: 22331464]
5. Liu B, Chen Y, St Clair DK. ROS and p53: a versatile partnership. Free radical biology & medicine. 2008; 44:1529–35. [PubMed: 18275858]
6. Bae I, Fan S, Meng Q, Rih JK, Kim HJ, Kang HJ, et al. BRCA1 induces antioxidant gene expression and resistance to oxidative stress. Cancer Res. 2004; 64:7893–909. [PubMed: 15520196]
7. Roy R, Chun J, Powell SN. BRCA1 and BRCA2: different roles in a common pathway of genome protection. Nat Rev Cancer. 2012; 12:68–78. [PubMed: 22193408]
8. Moynahan ME, Jasin M. Mitotic homologous recombination maintains genomic stability and suppresses tumorigenesis. Nature reviews. 2010; 11:196–207.
9. Xia B, Sheng Q, Nakanishi K, Ohashi A, Wu J, Christ N, et al. Control of BRCA2 cellular and clinical functions by a nuclear partner, PALB2. Mol Cell. 2006; 22:719–29. [PubMed: 16793542]
10. Tischkowitz M, Xia B. PALB2/FANCN: recombining cancer and Fanconi anemia. Cancer Res. 2010; 70:7353–9. [PubMed: 20858716]
11. Erkko H, Xia B, Nikkila J, Schleutker J, Syrjakoski K, Mannermaa A, et al. A recurrent mutation in PALB2 in Finnish cancer families. Nature. 2007; 446:316–9. [PubMed: 17287723]
12. Rahman N, Seal S, Thompson D, Kelly P, Renwick A, Elliott A, et al. PALB2, which encodes a BRCA2-interacting protein, is a breast cancer susceptibility gene. Nat Genet. 2007; 39:165–7. [PubMed: 17200668]
13. Reid S, Schindler D, Hanenberg H, Barker K, Hanks S, Kalb R, et al. Biallelic mutations in PALB2 cause Fanconi anemia subtype FA-N and predispose to childhood cancer. Nat Genet. 2007; 39:162–4. [PubMed: 17200671]
14. Xia B, Dorsman JC, Ameziane N, de Vries Y, Rooimans MA, Sheng Q, et al. Fanconi anemia is associated with a defect in the BRCA2 partner PALB2. Nat Genet. 2007; 39:159–61. [PubMed: 17200672]

15. Casadei S, Norquist BM, Walsh T, Stray S, Mandell JB, Lee MK, et al. Contribution of inherited mutations in the BRCA2-interacting protein PALB2 to familial breast cancer. Cancer Res. 2011; 71:2222–9. [PubMed: 21285249]
16. Jones S, Hruban RH, Kamiyama M, Borges M, Zhang X, Parsons DW, et al. Exomic sequencing identifies PALB2 as a pancreatic cancer susceptibility gene. Science (New York, NY. 2009; 324:217.
17. Zhang F, Ma J, Wu J, Ye L, Cai H, Xia B, et al. PALB2 links BRCA1 and BRCA2 in the DNA-damage response. Curr Biol. 2009; 19:524–9. [PubMed: 19268590]
18. Sy SM, Huen MS, Chen J. PALB2 is an integral component of the BRCA complex required for homologous recombination repair. Proc Natl Acad Sci U S A. 2009; 106:7155–60. [PubMed: 19369211]
19. Evers B, Jonkers J. Mouse models of BRCA1 and BRCA2 deficiency: past lessons, current understanding and future prospects. Oncogene. 2006; 25:5885–97. [PubMed: 16998503]
20. Rantakari P, Nikkila J, Jokela H, Ola R, Pylkas K, Lagerbohm H, et al. Inactivation of Palb2 gene leads to mesoderm differentiation defect and early embryonic lethality in mice. Hum Mol Genet. 2010; 19:3021–9. [PubMed: 20484223]
21. Bouwman P, Drost R, Klijn C, Pieterse M, van der Gulden H, Song JY, et al. Loss of p53 partially rescues embryonic development of Palb2 knockout mice but does not foster haploinsufficiency of Palb2 in tumour suppression. J Pathol. 2011; 224:10–21. [PubMed: 21404276]
22. Holstege H, Joosse SA, van Oostrom CT, Nederlof PM, de Vries A, Jonkers J. High Incidence of Protein-Truncating TP53 Mutations in BRCA1-Related Breast Cancer. Cancer Res. 2009
23. Greenblatt MS, Chappuis PO, Bond JP, Hamel N, Foulkes WD. TP53 mutations in breast cancer associated with BRCA1 or BRCA2 germ-line mutations: distinctive spectrum and structural distribution. Cancer Res. 2001; 61:4092–7. [PubMed: 11358831]
24. Ludwig T, Fisher P, Murty V, Efstratiadis A. Development of mammary adenocarcinomas by tissue-specific knockout of Brca2 in mice. Oncogene. 2001; 20:3937–48. [PubMed: 11494122]
25. Shakya R, Szabolcs M, McCarthy E, Ospina E, Basso K, Nandula S, et al. The basal-like mammary carcinomas induced by Brca1 or Bard1 inactivation implicate the BRCA1/BARD1 heterodimer in tumor suppression. Proc Natl Acad Sci U S A. 2008; 105:7040–5. [PubMed: 18443292]
26. Jonkers J, Meuwissen R, van der Gulden H, Peterse H, van der Valk M, Berns A. Synergistic tumor suppressor activity of BRCA2 and p53 in a conditional mouse model for breast cancer. Nat Genet. 2001; 29:418–25. [PubMed: 11694875]
27. Xu X, Wagner KU, Larson D, Weaver Z, Li C, Ried T, et al. Conditional mutation of Brca1 in mammary epithelial cells results in blunted ductal morphogenesis and tumour formation. Nat Genet. 1999; 22:37–43. [PubMed: 10319859]
28. Liu X, Holstege H, van der Gulden H, Treur-Mulder M, Zevenhoven J, Velds A, et al. Somatic loss of BRCA1 and p53 in mice induces mammary tumors with features of human BRCA1-mutated basal-like breast cancer. Proc Natl Acad Sci U S A. 2007; 104:12111–6. [PubMed: 17626182]
29. Cheung AM, Elia A, Tsao MS, Done S, Wagner KU, Hennighausen L, et al. Brca2 deficiency does not impair mammary epithelium development but promotes mammary adenocarcinoma formation in p53(+/−) mutant mice. Cancer Res. 2004; 64:1959–65. [PubMed: 15026330]
30. Shen SX, Weaver Z, Xu X, Li C, Weinstein M, Chen L, et al. A targeted disruption of the murine Brca1 gene causes gamma-irradiation hypersensitivity and genetic instability. Oncogene. 1998; 17:3115–24. [PubMed: 9872327]
31. Ludwig T, Chapman DL, Papaioannou VE, Efstratiadis A. Targeted mutations of breast cancer susceptibility gene homologs in mice: lethal phenotypes of Brca1, Brca2, Brca1/Brca2, Brca1/p53, and Brca2/p53 nullizygous embryos. Genes & development. 1997; 11:1226–41. [PubMed: 9171368]
32. Mizushima N, Komatsu M. Autophagy: renovation of cells and tissues. Cell. 2011; 147:728–41. [PubMed: 22078875]
33. Mathew R, Kongara S, Beaudoin B, Karp CM, Bray K, Degenhardt K, et al. Autophagy suppresses tumor progression by limiting chromosomal instability. Genes & development. 2007; 21:1367–81. [PubMed: 17510285]

34. Karantza-Wadsworth V, Patel S, Kravchuk O, Chen G, Mathew R, Jin S, et al. Autophagy mitigates metabolic stress and genome damage in mammary tumorigenesis. Genes & development. 2007; 21:1621–35. [PubMed: 17606641]
35. Mathew R, Karp CM, Beaudoin B, Vuong N, Chen G, Chen HY, et al. Autophagy suppresses tumorigenesis through elimination of p62. Cell. 2009; 137:1062–75. [PubMed: 19524509]
36. Yue Z, Jin S, Yang C, Levine AJ, Heintz N. Beclin 1, an autophagy gene essential for early embryonic development, is a haploinsufficient tumor suppressor. Proc Natl Acad Sci U S A. 2003; 100:15077–82. [PubMed: 14657337]
37. Qu X, Yu J, Bhagat G, Furuya N, Hibshoosh H, Troxel A, et al. Promotion of tumorigenesis by heterozygous disruption of the beclin 1 autophagy gene. The Journal of clinical investigation. 2003; 112:1809–20. [PubMed: 14638851]
38. Guo JY, Chen HY, Mathew R, Fan J, Strohecker AM, Karsli-Uzunbas G, et al. Activated Ras requires autophagy to maintain oxidative metabolism and tumorigenesis. Genes & development. 2011; 25:460–70. [PubMed: 21317241]
39. Yang S, Wang X, Contino G, Liesa M, Sahin E, Ying H, et al. Pancreatic cancers require autophagy for tumor growth. Genes & development. 2011; 25:717–29. [PubMed: 21406549]
40. White E. Deconvoluting the context-dependent role for autophagy in cancer. Nat Rev Cancer. 2012; 12:401–10. [PubMed: 22534666]
41. Kimmelman AC. The dynamic nature of autophagy in cancer. Genes & development. 2011; 25:1999–2010. [PubMed: 21979913]
42. Bowman-Colin C, Xia B, Bunting S, Klijn C, Drost R, Bouwman P, et al. Palb2 synergizes with Trp53 to suppress mammary tumor formation in a model of inherited breast cancer. Proc Natl Acad Sci U S A. 2013
43. Wagner KU, Wall RJ, St-Onge L, Gruss P, Wynshaw-Boris A, Garrett L, et al. Cre-mediated gene deletion in the mammary gland. Nucleic acids research. 1997; 25:4323–30. [PubMed: 9336464]
44. Buisson R, Dion-Cote AM, Coulombe Y, Launay H, Cai H, Stasiak AZ, et al. Cooperation of breast cancer proteins PALB2 and piccolo BRCA2 in stimulating homologous recombination. Nat Struct Mol Biol. 2010; 17:1247–54. [PubMed: 20871615]
45. Young AR, Narita M, Ferreira M, Kirschner K, Sadaie M, Darot JF, et al. Autophagy mediates the mitotic senescence transition. Genes & development. 2009; 23:798–803. [PubMed: 19279323]
46. Heikkinen T, Karkkainen H, Aaltonen K, Milne RL, Heikkila P, Aittomaki K, et al. The breast cancer susceptibility mutation PALB2 1592delT is associated with an aggressive tumor phenotype. Clin Cancer Res. 2009; 15:3214–22. [PubMed: 19383810]
47. Diaz-Cruz ES, Cabrera MC, Nakles R, Rutstein BH, Furth PA. BRCA1 deficient mouse models to study pathogenesis and therapy of triple negative breast cancer. Breast Dis. 2010; 32:85–97. [PubMed: 21778574]
48. Tasdemir E, Chiara Maiuri M, Morselli E, Criollo A, D'Amelio M, Djavaheri-Mergny M, et al. A dual role of p53 in the control of autophagy. Autophagy. 2008; 4:810–4. [PubMed: 18604159]

Significance

Our findings directly demonstrate a tumor-promoting role of autophagy in a new model of hereditary breast cancer. Given the close functional relationship and the genetic similarity between PALB2 and BRCA1/2, our results further suggest that inhibition of autophagy may represent a new avenue to the prevention or treatment of a significant portion of hereditary breast cancers, namely ones associated with DNA damage and oxidative stress.

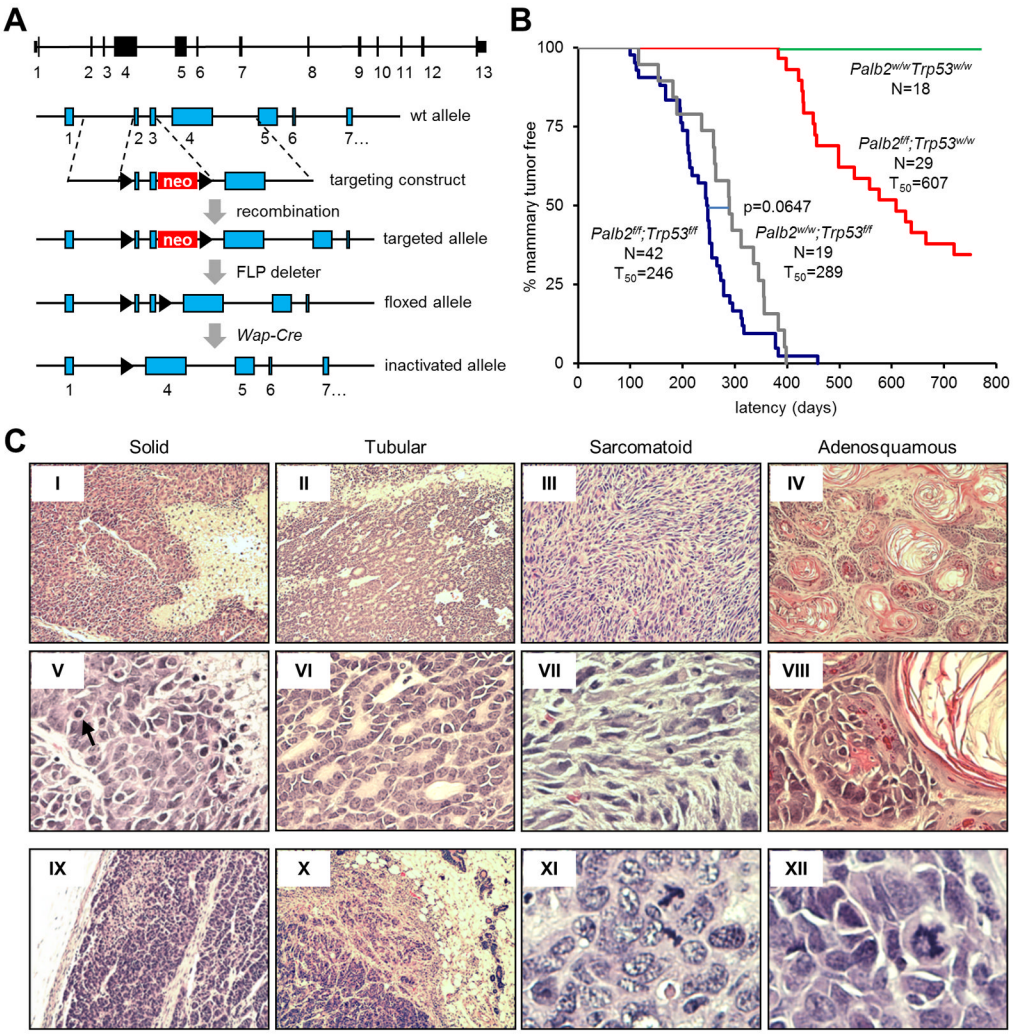

Figure 1.

Mammary tumor development in mice with tissue-specific ablation of *Palb2*. **A,** Schematic representation of the generation of the *Palb2*-floxed and knockout alleles. The full gene structure of *Palb2* is shown on top. **B,** Kaplan-Meier survival curves of mice with mammary gland-specific deletion of *Palb2*, *Trp53* or both genes. **C,** Diverse histology of *Palb2*-associated mouse mammary tumors. I-IV, the 4 different types of histology observed; V-VIII, enlarged views of the center regions of I-IV, respectively; IX, a solid tumor with a well-formed pushing margin; X, a solid tumor invading into fat tissue; XI-XII, higher power views of tumor cell nuclei and mitotic figures.

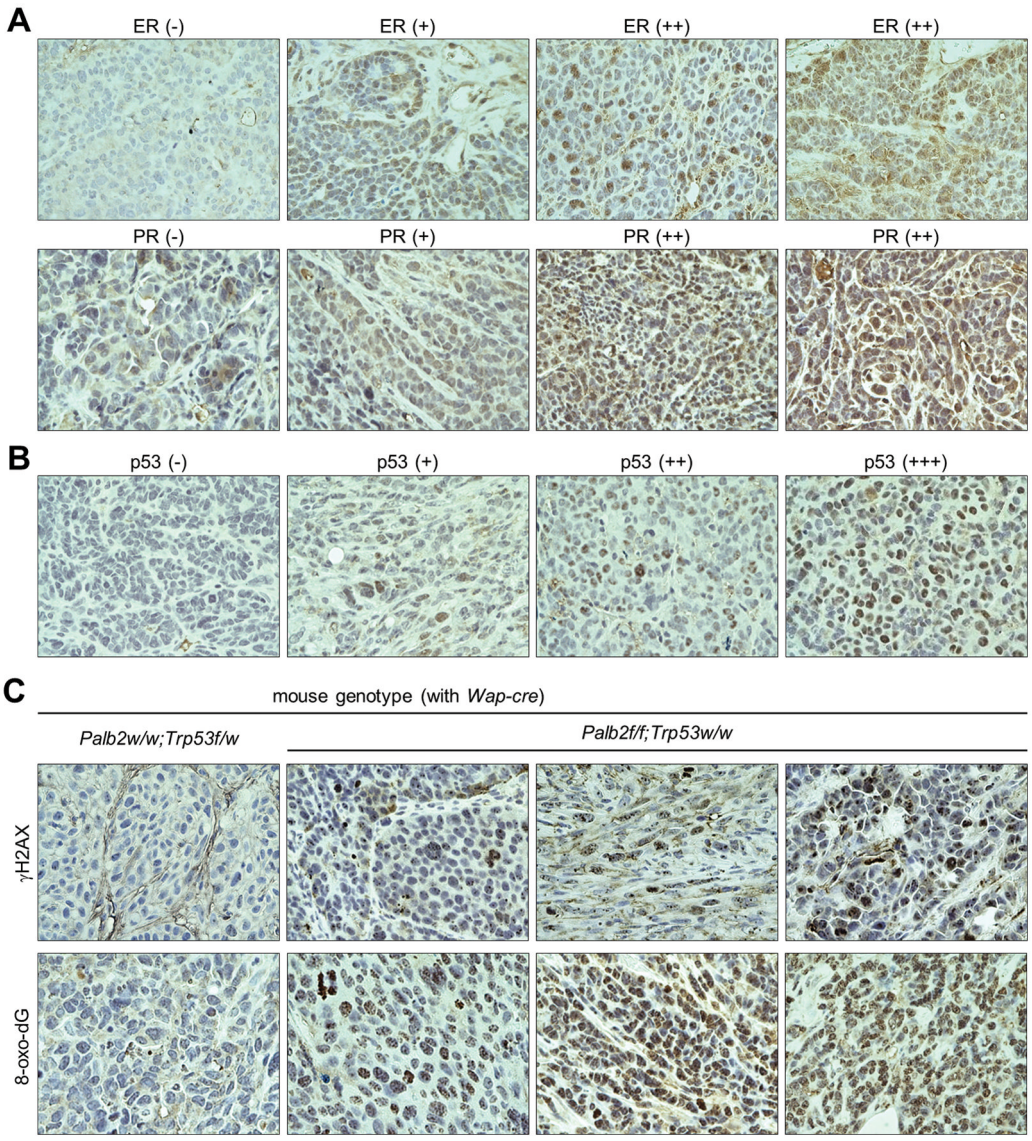

Figure 2.

Characterization of *Palb2*-asscoiated mouse mammary tumors by IHC. **A**, Representative ER and PR staining patterns of the tumors. Since similar percentage of staining- positive cells were found in most of the positive tumors, assignment of "+" or "++" grades is purely based on the intensity of staining signals. **B**, Representative staining patterns of p53 in the tumors. Grade assignment is based on the relative staining intensity. **C**, Different staining patterns of γH2A.X. (upper panels) and 8-oxo-dG (lower panels) in the control and *Palb2*-null tumors.

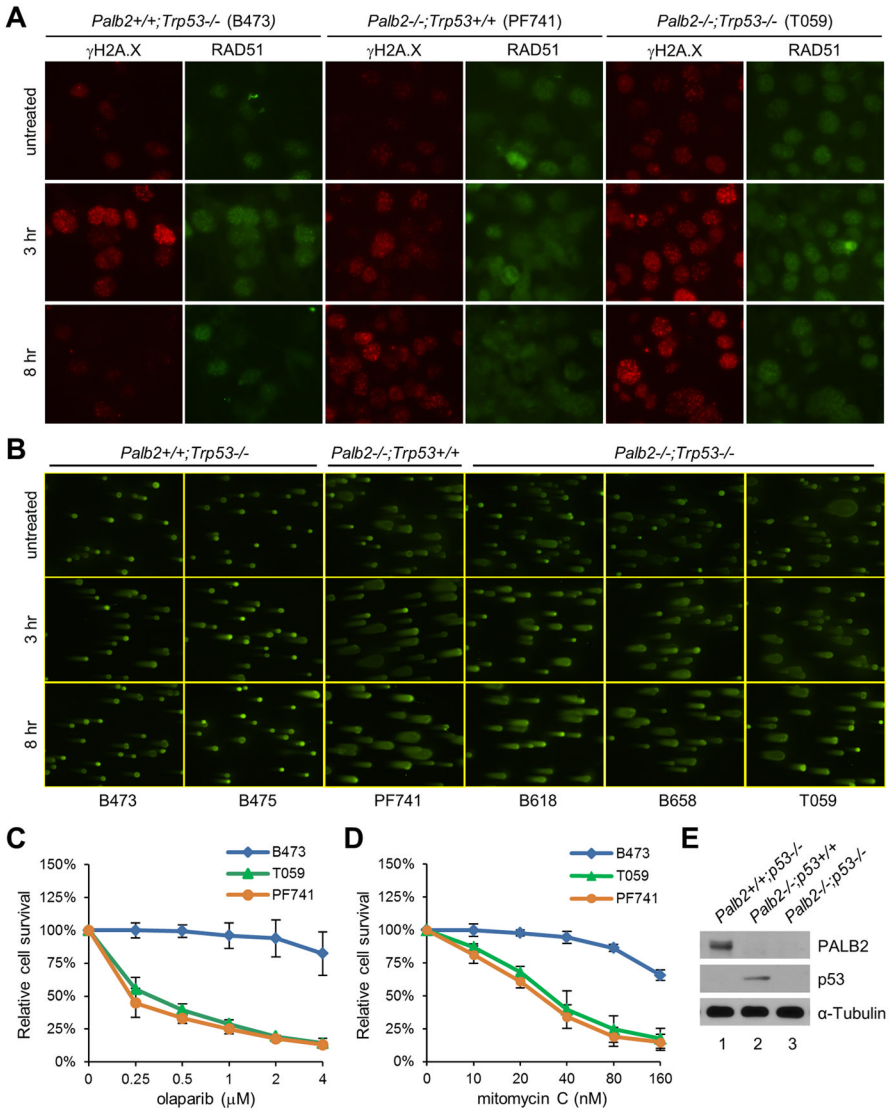

Figure 3.

DNA repair defect of *Palb2*-null tumor cells. **A**, γH2A.X and RAD51 foci formation before and after DNA damage induced by olaparib. Tumors cells were treated with 25 μM olaparib for 1 hr and the drug was then removed. Cells were fixed at 3 and 8 hr after drug removal and analyzed by IF. **B**, Levels of DNA breaks before and after olaparib treatment. Cells were treated as above, collected at the same time points and analyzed by neutral comet assay. **C–D**, Sensitivity of the tumor cells to olaparib and MMC. Cells were seeded in 96-well plates, treated with the drugs for 4 days and analyzed by CellTiterGlo assay. **E**, Western blots showing PALB2 and p53 protein levels in the tumor cells analyzed in **C**–**D**.

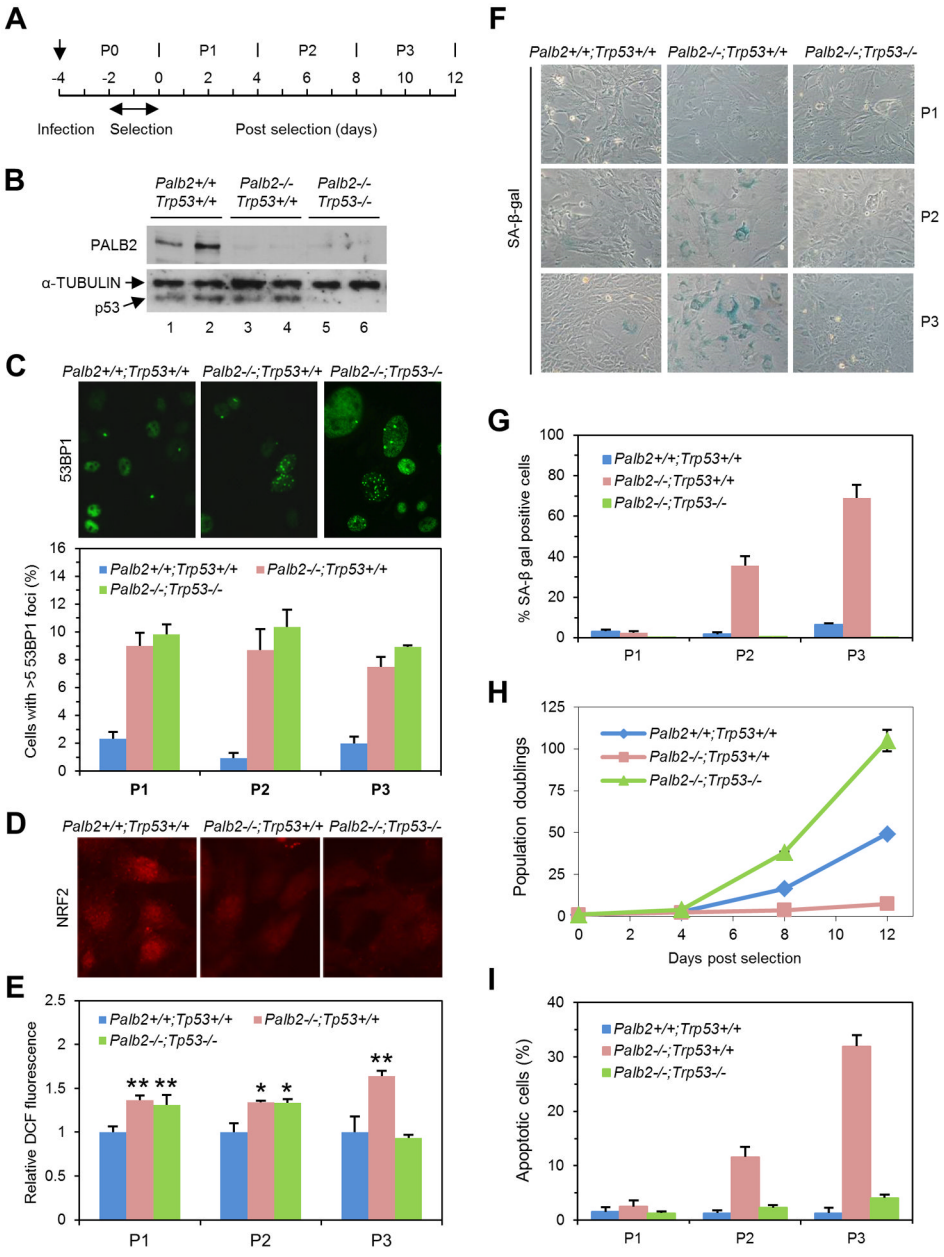

Figure 4.

Senescence and apoptosis of mouse embryonic fibroblasts (MEFs) following *Palb2* loss and the rescue by co-deletion of *Trp53*. **A,** Schematic timeline of the generation and passaging of the MEFs. Two different MEF lines of each genotype were generated and analyzed in parallel. **B,** Western blots showing loss of PALB2, p53 or both proteins in the MEFs at passage 2. **C,** 53BP1 nuclear foci formation in the control, *Palb2* deletion and *Palb2*/*Trp53* double deletion MEFs. The top panel shows representative immunofluorescence (IF) images of 53BP1 staining during passage 1, and the bottom panel shows quantification of foci-positive cells in all 3 passages. **D,** NRF2 localization in the MEFs during passage 1, as determined by IF. **E,** Cellular levels of reactive oxygen species (ROS) in the MEFs in all 3 passages. **F–G,** Cellular senescence induced by *Palb2* inactivation and the rescue by co-deletion of *Trp53*. **F** shows representative images of beta-galactosidase (β-gal) staining of

the wild type, *Palb2*-null and *Palb2*/*Trp53*-double-null MEFs, and the quantification is shown in **G. H,** Growth curves of the MEFs showing the growth arrest of the *Palb2*-null MEFs and the rescue by loss of p53. **I,** Cellular apoptosis following *Palb2* inactivation and the rescue by co-deletion of *Trp53*. Apoptotic cells were measured by Annexin V assay. In all above analyses, values shown are the averages of the 2 independent MEFs lines for each genotype and error bars represent standard deviations. P values were determined by two-tailed *t*-test. *$p \leq 0.05$; **$p \leq 0.01$.

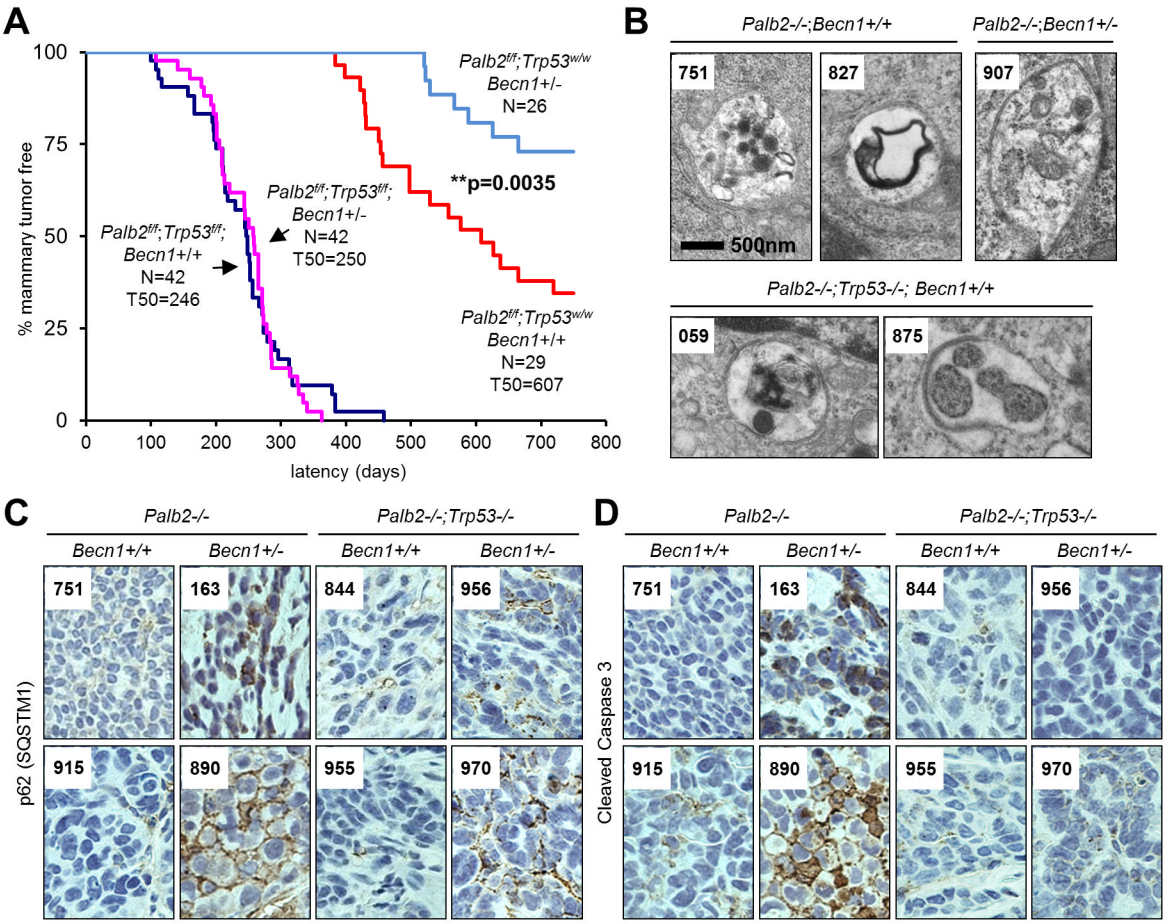

Figure 5.

Role of autophagy in *Palb2*-associated mammary tumor development. **A,** Kaplan-Meier survival curves showing mammary tumor development in *Palb2*-single and *Palb2;Trp53*-double conditional knockout mice in *Becn1*$^{+/+}$ and *Becn1*$^{+/-}$ backgrounds. **B,** Autophagosomes observed in tumors from mice with indicated genotypes. Note that tumor #827 contains a *Trp53* point mutation (Table 1), although it developed in *Trp53*-wild type mice. **C,** IHC analysis of autophagy substrate p62 in tumors arising from the 4 different genetic backgrounds as indicated. Tumors #751 and #163 still retained wild type *Trp53*, whereas #915 and #890 had acquired somatic mutations in *Trp53* (Table 1). **D,** IHC analysis of cleaved caspase 3, a marker of apoptosis, in the same tumors as in **C**.

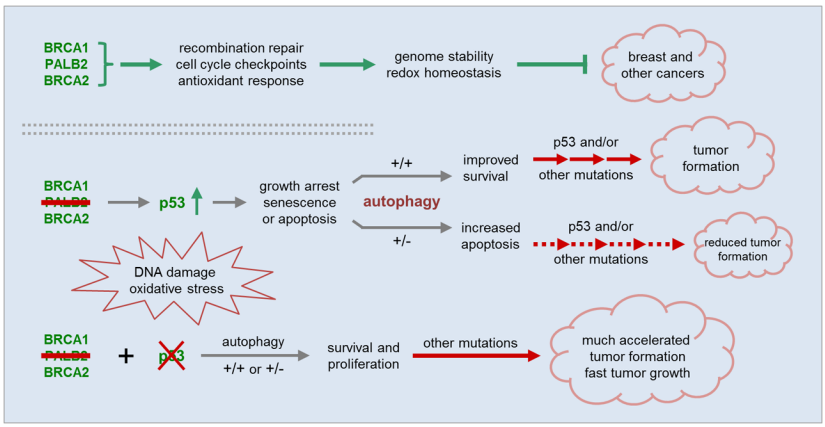

Figure 6.

A model of the developmental paths of *PALB2*-associated breast cancer. Under normal conditions, PALB2 functions together with BRCA1 and BRCA2 to maintain genome stability and cellular homeostasis to suppress cancer development. Upon loss of PALB2, p53 is activated posing a strong barrier to tumor formation, whereas autophagy helps sustain cell viability and proliferation thereby facilitating tumor cell evolution. However, the impact of autophagy may only manifest when p53 is functional.

Table 1

Characteristics of mammary tumors developed in *Palb2* CKO mice with *Becn1*$^{+/+}$ and *Becn1*$^{+/-}$ backgrounds

See Figure 1 for definitions and examples of histology and ER, PR and p53 immuno grades. "±" indicates weak staining in only some areas of the tumors. For γH2A.X, "+++", "++" and "+" denote tumors in which ≥30%, 10–30% and 1–10% of cells, respectively, show 3 strongly stained foci or virtually pan-nuclear staining; "SF" denotes tumors in which a single, large focus was observed per cell, which is possibly the inactivated X chromosome. Grade assignment for 8-oxo-dG staining is based on the relative staining intensity, as all positive tumors have greater than 60% of cells showing positive staining. *Trp53* mutations are shown at both DNA and protein levels, separated by a forward slash. N.D., *Trp53* cDNA sequence not determined due to poor quality of RNA isolated from frozen tissues.

Mouse ID	*Becn1*	Latency	Tumor	Histology (H&E)	Immunohistochemistry					*Trp53* mutation
					ER	PR	γH2A.X	8-oxo-dG	p53	
914	+/+	383	1	Solid+Tubular	++	++	+++	+++	+++	G809A/R270H
949	+/+	398	1	Solid+Tubular	+	−	++	+++	+++	G720A/M240I, G721T/G241W
741	+/+	422	1	Sarcomatoid+Tubular	++	++	++	+++	−	WT
749	+/+	428	1	Solid+Tubular	+	−	SF	+++	−	Δ985–1089
826	+/+	430	1	Solid→Sarcomatoid	+	−	+	+++	−	N.D.
824	+/+	431	1	Solid+Tubular	+	−	+++	+++	+++	T391C/F131L
808	+/+	450	1	Sarcomatoid+Tubular	−	−	−	+++	−	N.D.
882	+/+	453	1	Solid+Tubular	−	+	+++	++	+++	WT
751	+/+	456	1	Tubular+Solid	−	−	SF	−	−	WT
049	+/+	498	1	Solid+Tubular	−	−	+++	+++	−	Δ541–546, Δ664–771
912	+/+	498	1	Solid→Sarcomatoid	++	−	+++	+++	+++	C808T/R270C
915	+/+	529	1	Solid+Tubular	−	−	++	+	+++	A632G/H211R
742	+/+	576	1	Squamous+Tubular	+	++	−	+++	−	N.D.
827	+/+	608	T1	Solid+Tubular	−	−	+	++	+++	G829A/R277G
	+/+	608	T2	Solid+Tubular	−	−	+	−	+++	N.D.
825	+/+	637	1	Solid+Tubular	−	−	+	+++	−	WT
042	+/+	665	1	Squamous+Tubular	−	−	−	++	−	no PCR product
747	+/+	719	1	Sarcomatoid+Solid	−	−	+++	+++	+	T618A/V206D
907	+/−	520	1	Solid+Tubular	−	−	SF	+	−	WT
163	+/−	522	1	Solid+Tubular	−	++	+++	+++	−	WT
890	+/−	529	T1	Solid	−	−	++	++	+++	C404T/A135V

Mouse ID	*Becn1*	Latency	Tumor	Histology (H&E)	Immunohistochemistry					*Trp53* mutation
					ER	PR	γH2A.X	8-oxo-dG	p53	
	+/−	529	T2	Squamous+Tubular	−	−	SF	++	−	N.D.
047	+/−	567	1	Squamous+Solid+Tubular	−	−	−	+	−	N.D.
723	+/−	588	1	Solid+Tubular	±	−	+++	+++	−	WT
119	+/−	626	1	Solid+Tubular	±	+	+	+++	−	WT
153	+/−	665	1	Tubular+Solid	−	−	+	+	++	WT